

## 7.1 HIGH-RESOLUTION MODELING OF THE NIGHTTIME BOUNDARY LAYER EVOLUTION IN THE OWENS VALLEY: COMPARISON TO OBSERVATIONS

Jürg Schmidli, Gregory Poulos  
Earth Observing Laboratory, NCAR, Boulder, Colorado

### 1 INTRODUCTION

The boundary layer in mountainous terrain is characterized by a high degree of complexity. On days with weak synoptic and sufficient radiative forcing, thermally-induced flows of various scales develop, including local slope flows, cross-valley circulations, thermally-induced valley flows, and regional-scale mountain-plain winds (*Whiteman, 2000*). These flows interact with each other and with the small-scale turbulent processes. Due to these highly non-linear interactions our understanding of the boundary layer over complex terrain is still fairly limited. However, a better understanding of these processes is necessary in order to improve the representation of the atmospheric boundary layer in numerical weather prediction and climate models (*Rotach et al., 2004*). A crucial process which has to be better characterized in order to improve models of the stable boundary layer (in flat and mountainous terrain) is intermittent turbulence (*Nappo, 1991; McNider et al., 1995; Mahrt, 1998; Derbyshire, 1999; Poulos and Burns, 2003*).

We use large-eddy simulations (LES) for the investigation of thermally-induced flows and possible sources of intermittent turbulence in the nocturnal valley atmosphere. As our simulation tool we use the Advanced Regional Prediction System (ARPS *Xue et al., 2000, 2001*). We have chosen the Owens Valley in California for simulation, where during the recent Terrain-induced Rotors Experiment (T-REX, held 1 March - 30 April 2006, near Independence, CA) extensive observations of the mountain boundary layer were taken. Instrument systems deployed include wind profilers with radio acoustic sounding systems, aerosol and doppler lidars, radio soundings, three 30 m flux towers, and many more.

We have chosen EOP2 (29/30 March 2006) of the T-REX field campaign for simulation. EOP2 is characterized by the passage of a weak short-wave high-pressure ridge with some high cirrus clouds during the night (maximum surface pressure at Independence is reached at about 15 UTC on 30 March). The above-ridge-level winds remain fairly constant at about 15-20 m/s while turning from NW to W during the night. Here we use the ARPS simulations to elaborate on the three-dimensional flow structure in the valley and to identify possible sources of intermittent turbulence. The characteristics of near-surface tur-

bulence as measured by three 30 m flux towers are investigated in more detail in the companion paper (*Poulos and Schmidli, 2006*).

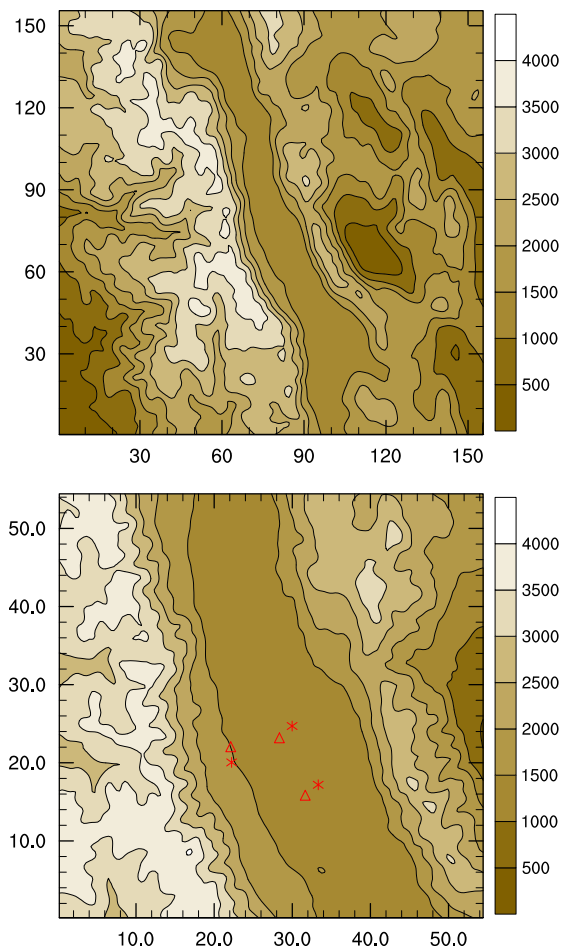


Figure 1: Topography of the Owens Valley and location of the ISFF flux towers (asterisks) and the ISS wind profilers (triangles); Elevation contours for the 1km grid (top) and the 350m grid (bottom).

### 2 SIMULATION SETUP

ARPS is applied in a one-way nesting mode, forced by the NAM analysis and nested down to 350 m horizontal resolution. The setup is similar to that of *Chow et al. (2006)* and *Weigel et al. (2006)*. Key simulation parameters of each grid level are listed in Table 1.

The topography for the coarser (finer) two grids was obtained from the USGS 30 (3) arc second topography dataset.

Table 1: Simulation parameters for the four grids.

(nx,ny,nz)	$\Delta h$	$\Delta z_{min}/\Delta z_{avg}$	$\Delta t/\Delta \tau$
(135,135,53)	9 km	50/500 m	10/10 s
(135,135,53)	3 km	50/500 m	2/2 s
(159,159,63)	1 km	40/400 m	1/1 s
(159,159,71)	350 m	30/350 m	1/0.2 s

For surface characteristics we use the standard ARPS soil types and vegetation type classes. The 1 km soil type dataset is based on the state soil geographic (STATSGO) database, the 1 km vegetation type and NDVI datasets are based on the 1 km USGS North American datasets. From this input datasets ARPS derives the leaf area index (LAI), surface roughness ( $z_0$ ), and the vegetation fraction used by the land-surface soil-vegetation model.

Initial and boundary conditions required to drive the 9 km run were derived from NAM analyses obtained through NOMADS. Simulations were carried out for 42 hours beginning at 12 UTC on 29 March. Output was stored at hourly intervals and used to force the subsequent nested grid simulations.

The coarse-resolution (14 km) surface data from NAM was found to be inadequate for our simulations

(for instance, there was snow down in Owens Valley in the analysis, although the observed snowline was somewhere between 2500 and 3000 m). Therefore we initialized the simulations as follows: Soil temperature for all grids was set equal to the near-surface temperature, soil moisture was set to a constant soil saturation rate, and the snow cover was set to zero. In order to investigate the effect of soil moisture on the flow different values of soil saturation rate were used (see Table 2).

For the physical parameterizations standard ARPS options were used (Xue *et al.*, 2001): a 1.5-order TKE turbulence closure model to represent turbulent mixing (Deardorff, 1980; Moeng, 1984), stability and roughness-length dependent surface fluxes (Businger *et al.*, 1971; Byun, 1990), a force-restore two-layer soil-vegetation model based on Noilhan and Planton (1989), and a sophisticated radiation package developed at NASA/Goddard Space Flight Center.

Table 2: Simulation configurations, where SAT denotes soil moisture saturation rate.

Name	Configuration
REF	reference simulation; SAT=20%
DRY	dry soil run; SAT=10%
MOIST	moist soil run; SAT=50%
NORAD	run with no radiative forcing

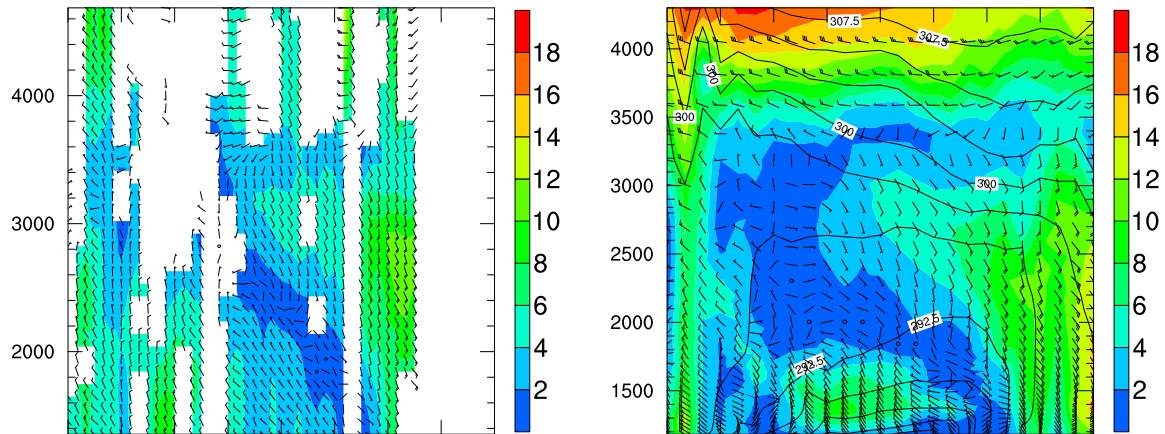


Figure 2: Meteorogram of wind direction (barbs), wind velocity (color) and potential temperature (contour lines) at the MISS Manzanar site for the wind profiler (a, left panel) and the model simulation (b, right panel).

### 3 THE FLOW STRUCTURE

#### 3.1 Observations

From the wind profilers and the radiosonde data the following picture of the flow structure and evolution in Owens Valley can be deduced. During most of the day of the 29th the winds in the valley are weak

(2-4 m/s, not shown). During the nighttime a persistent downvalley flow develops at the Manzanar site (as shown in Fig 2a). The speed of the flow is typically about 4 m/s, with a peak strength of 8-10 m/s around 6 UTC. The depth of the downvalley flow layer is reduced from more than 1 km during the early night hours to less than a few hundred meters

by sunrise. Starting as early as 9 UTC a layer of southerly flow develops at higher elevations within the valley atmosphere (around 3000 m MSL), and increases in depth and strength throughout the night. Above ridge level the wind increases in strength and turns to westerly. The three-layer structure of a low-level northerly flow, a mid-level southerly flow, and a synoptic north-westerly flow is also evident from the radiosonde data (Fig 3a).

In the late afternoon the thermal structure of the valley is characterized by a well-mixed layer ( $\theta \sim 296$  K) reaching 4000 m MSL. During the night, a surface inversion is formed, and the upper-level inversion increases in strength and sinks to below 3500 m MSL (Fig 3b).

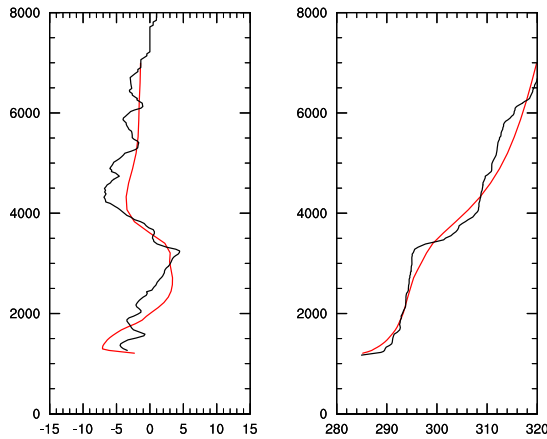


Figure 3: Observed radiosonde (black line) and simulated (red line) profiles of meridional velocity (a, left panel) and potential temperature (b, right panel) at 11 UTC.

### 3.2 Simulation

Our simulations with ARPS are able to reproduce all the observed features. Figure 2 shows a comparison of the observed and simulated evolution of the valley flow at the Manzanar site during the night and the following day (until 4 pm PST). The three-layer structure with the downward propagation of the southerly flow layer is clearly reproduced. While the strength of the southerly flow is captured very well, the strength of the katabatic downvalley flow is somewhat overestimated by the model and its depth is slightly underestimated. This finding is supported by comparison with the radiosonde data (Figure 3a).

With regards to the thermal structure of the valley atmosphere, the model is able to reproduce the surface inversion (albeit the simulated surface inversion layer is a bit too deep). The upper-level inversion, however, is not well captured by the model, likely

due to insufficient vertical resolution (the vertical grid spacing at the inversion height is about 250 m).

What is the evolution and three-dimensional structure of the flow according to the model? Can potential sources of intermittent turbulence be identified? According to the model simulation two quite different phases can be distinguished. During the evening hours (around 2 UTC) strong katabatic flows emerge from the major side-valleys producing a highly complex flow pattern and significant turbulence within the valley (not shown). For instance, the velocity of the simulated Onion Valley jet exceeds 10 m/s. During a second phase, starting around 6 UTC, a more or less steady katabatic downvalley flow is established and persists throughout the rest of the night (Figure 4). With the downvalley jet a quasi-stationary mesoscale eddy forms near the ISFF towers (at 14 UTC the eddy is just north of the central tower). Clearly these evolving mesoscale features are a potential source of the intermittent turbulence events observed in the near-surface atmosphere (*Poulos and Schmidli, 2006*). Analysis of additional observations will be required in order to confirm or refute the existence of these mesoscale features.

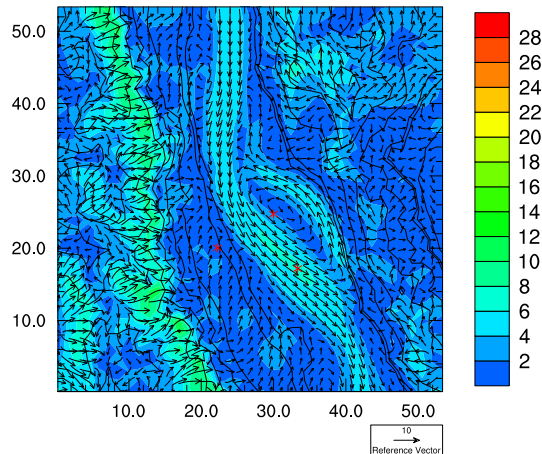


Figure 4: Wind speed and wind vectors at 14 UTC at a height of 1400 m over the valley and on the lowest model level over higher topography respectively.

To what height is the valley atmosphere influenced by thermally-induced flows? Figure 5 shows a comparison between the reference simulation and a simulation with no radiative forcings and no surface fluxes (NORAD). Above about 2500 m MSL the two simulation are very similar. This means, that the flow above this level is determined mainly by the large-scale synoptic forcing, while the lower-level flow is forced by radiative cooling of the near-surface atmosphere.

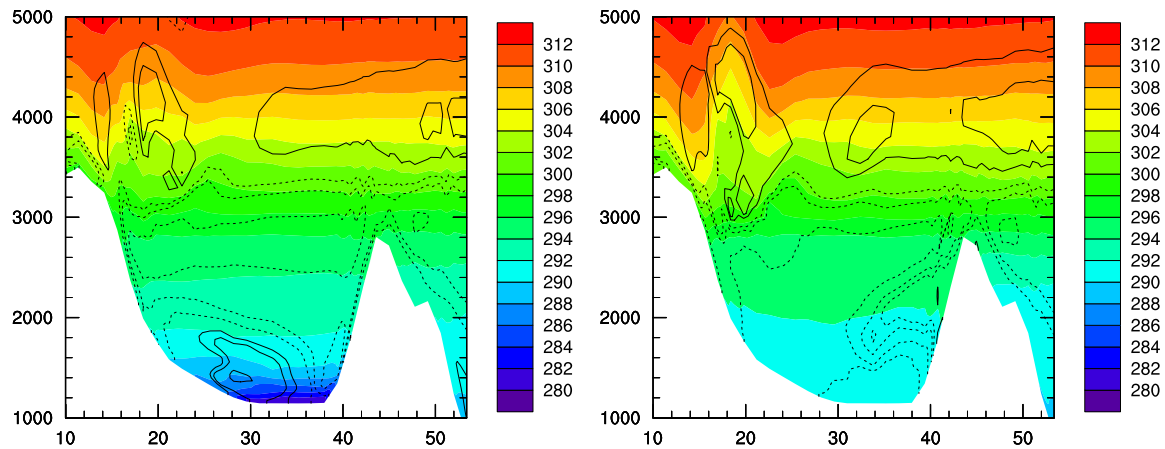


Figure 5: Along-valley wind component (contour lines) and potential temperature (filled contours) in a valley cross-section at the height of the western ISFF flux tower at 14 UTC for REF (a, left panel) and NORAD (b, right panel).

#### 4 EVOLUTION OF NEAR-SURFACE FIELDS

Observations of wind and temperature, turbulent fluxes of momentum, sensible and latent heat, as well as all radiation components, taken at the three ISFF flux towers, complement the picture of the valley flow evolution. In this section we compare some of these measurements with the tree simulations (REF, DRY, and MOIST), for further analyses see *Poulos and Schmidli (2006)*.

Figure 6 shows a comparison of observed and simulated near-surface wind speed (6a) and friction velocity (6b) during EOP2 at the southern ISFF flux tower. The diurnal variation of wind speed and momentum flux is clearly reproduced. However, all simulations tend to overestimate the average nighttime wind speed and underestimate the average daytime wind speed and friction velocity. The underestimation of the daytime velocity and turbulence intensity is largest for the moist simulation.

Figure 7 shows a comparison of observed and simulated near-surface temperature (7a) and sensible heat flux (7b). Again the diurnal variation of temperature and sensible heat flux is well reproduced by the model. However, the reference simulation builds up a cold bias during the night which reaches about 3 K before sunrise. While the downward sensible heat flux is overestimated during the night, the simulated daytime sensible heat flux is very close to the

observed value. Comparing the three simulations, it can be seen that the difference in the simulated sensible heat flux is small during the night and large during the day. This is to be expected from the known influence of soil moisture on the partitioning of the available energy between sensible and latent heat flux.

A detailed comparison of the observed and simulated surface energy and radiation budget has been carried out (not shown). The main findings can be summarized as follows:

- **Nighttime:** Simulated net longwave radiation is too negative mainly due to an underestimation of incoming longwave radiation by about 20-40 W/m<sup>2</sup>.
- **Daytime:** Simulated net radiation is about 30% too low mainly due to an underestimation of incoming shortwave radiation (about 20%), but also due to an overestimation of outgoing shortwave radiation (about 10%).
- The simulated sensible heat flux is close to the observations during the day, but it is overestimated during the night.
- The latent heat flux during the day is smaller than observed (for REF and DRY). The MOIST simulation largely overestimated the latent heat flux during the day and the night.

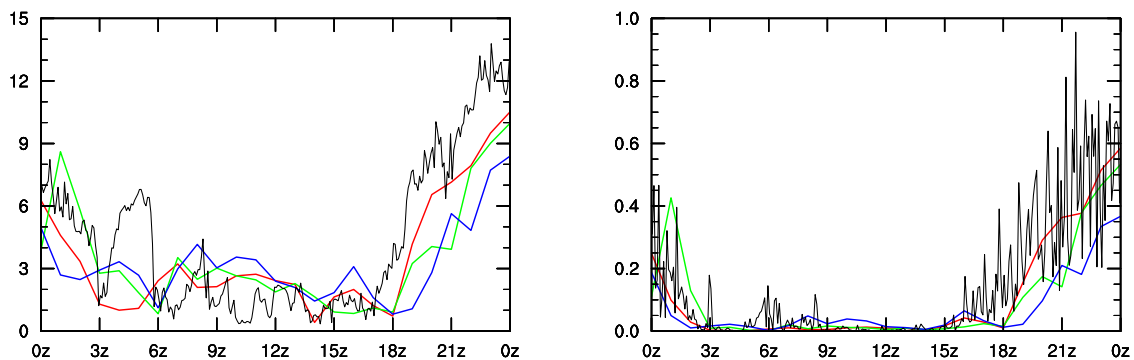


Figure 6: Observed (black) and simulated (color) time series of wind speed (a, left) and friction velocity (b, right) at 20 m height at ISFF south on 30 March. Results for three simulations are shown: DRY (red), REF (green), and MOIST (blue). Note that the observed series are based on 5 minute averages, whereas the simulated series are based on instantaneous model values, one per hour.

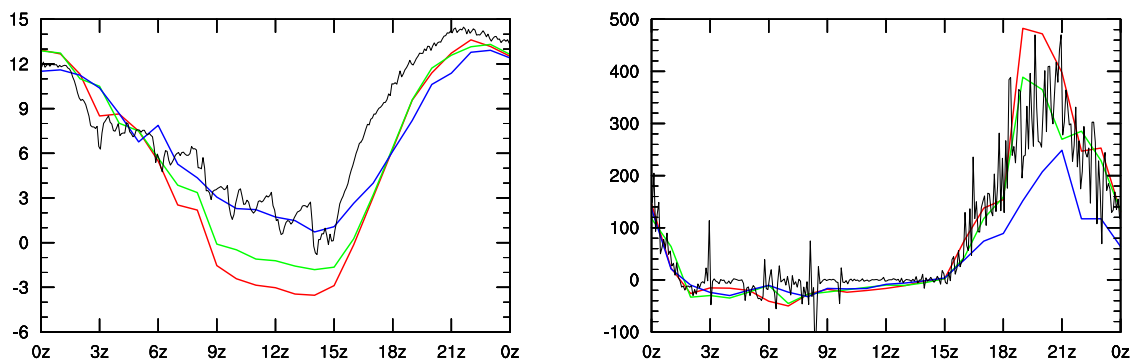


Figure 7: As in Figure 6, but for temperature (a, left) and sensible heat flux (b, right).

## 5 CONCLUSIONS

The evolution of the nighttime boundary layer in a deep valley during a period of weak to moderate synoptic forcing has been evaluated by comparing ARPS simulations with T-REX observations. The main findings so far can be summarized as follows:

- Despite the presence of a high cirrus cloud layer during most of the night, significant katabatic flows developed in the valley. The downvalley jet, as observed by one of the wind profilers, attained a maximum strength of 8-10 m/s around 6 UTC before weakening to 3-4m/s by the early morning hours. The downvalley jet was restricted to the lowest 1000 m above the valley floor. At mid-levels (2000-3000 m MSL) a southerly flow started to develop around 9 UTC and strengthened during the night.
- A highly variable flow evolution was evident at the tall flux towers located at the valley bottom and on the alluvial slope on the western valley sidewall. Inversion strength varied from near 0K/km to 120K/km in the lowest 30m above

ground. Surface fluxes of momentum and sensible heat varied by several orders of magnitude.

- The results from the ARPS simulations are very encouraging. The major features of the observed flow evolution can be reproduced. Comparison with the wind profilers, for instance, reveals remarkable agreement. The main shortcomings of the simulations appear to be the overestimation of the strength of the downvalley flow and the overestimation of the depth of the surface inversion layer. The former is likely due to a too high surface sensible heat flux, which is probably related to missing high-level clouds in the simulation. However, the surface layer parameterization, soil moisture initialization, and the turbulence scheme might also be contributing to the error.
- Sensitivity tests showed that the simulated flow is quite sensitive to soil moisture. Therefore good soil moisture initialization is an important step towards achieving accurate simu-

lations, also in Owens Valley (Chow et al 2006, Weigel et al 2006).

- Several possible sources of intermittent turbulence were identified, including tributary katabatic flows, semi-permanent deep valley vortices, and shear between down and upvalley flows.

#### ACKNOWLEDGEMENTS

The support of the Swiss National Science Foundation (grant PA002-111427) for the first author is gratefully acknowledged. The National Center for Atmospheric Research funded by NSF for the computing time used in this research. The ground-based instruments teams from the university community and NCAR for their outstanding efforts at T-REX. Andreas Weigel for providing access to his Riviera simulations.

#### REFERENCES

- Businger, J. A., J. C. Wyngaard, Y. Izumi, and E. F. Bradley (1971), Flux-profile relationships in the atmospheric surface layer, *J. Atmos. Sci.*, *28*, 181–189.
- Byun, D. W. (1990), On the analytical solutions of flux-profile relationships for the atmospheric surface layer, *J. Appl. Meteorol.*, *29*, 652–657.
- Chow, F. K., A. P. Weigel, R. L. Street, M. W. Rotach, and M. Xue (2006), High-resolution large-eddy simulations of flow in a steep Alpine valley. part i: Methodology, verification, and sensitivity experiments, *J. Appl. Meteorol.*, *45*, 63–86.
- Deardorff, J. W. (1980), Stratocumulus-capped mixed layers derived from a 3-dimensional model, *Boundary-Layer Met.*, *18*, 495–527.
- Derbyshire, S. H. (1999), Boundary-layer decoupling over cold surfaces as a physical boundary instability, *Boundary-Layer Met.*, *90*, 297–325.
- Mahrt, L. (1998), Stratified atmospheric boundary layers and breakdown of models, *Theoret. Comput. Fluid Dynamics*, *11*, 263–279.
- McNider, R. T., D. E. England, M. J. Friedman, and X. Shi (1995), Predictability of the stable atmospheric boundary layer, *J. Atmos. Sci.*, *52*, 1602–1623.
- Moeng, C.-H. (1984), A large-eddy simulation model for the study of planetary boundary-layer turbulence, *J. Atmos. Sci.*, *41*, 2052–2062.
- Nappo, C. (1991), Sporadic breakdowns of stability in the pbl over simple and complex terrain, *Boundary-Layer Met.*, *54*, 69–87.
- Noilhan, J., and S. Planton (1989), A simple parameterization of land surface processes for meteorological models, *Mon. Wea. Rev.*, *117*, 536–549.
- Poulos, G. S., and S. P. Burns (2003), An evaluation of bulk ri-based surface layer flux formulas for stable and very stable conditions with intermittent turbulence, *J. Atmos. Sci.*, *60*, 2523–2537.
- Poulos, G. S., and J. Schmidli (2006), Turbulence in the stable near-surface atmosphere in the complex terrain of Owens Valley, CA during T-REX, in *12th Conference on Mountain Meteorology*, Proc., Santa Fe, NM, August.
- Rotach, M. W., P. Calanca, G. Graziani, and Coauthors (2004), Turbulence structure and exchange processes in an alpine valley: The Riviera project, *Bull. Amer. Meteor. Soc.*, *85*, 1367–1385.
- Weigel, A. P., F. K. Chow, M. W. Rotach, R. L. Steet, and M. Xue (2006), High-resolution large-eddy simulations of flow in a steep Alpine valley. part ii: Flow structure and heat budgets, *J. Appl. Meteorol. and Climatol.*, *45*, 87–107.
- Whiteman, C. D. (2000), *Mountain Meteorology: Fundamentals and Applications*, 355 pp., Oxford University Press.
- Xue, M., K. K. Droegemeier, and V. Wong (2000), The advanced regional prediction system (arps) — a multi-scale nonhydrostatic atmospheric simulation and prediction model. part i: Model dynamics and verification, *Meteorol. Atmos. Phys.*, *75*, 161–193.
- Xue, M., K. K. Droegemeier, V. Wong, A. Shapiro, K. Brewster, F. Carr, D. Weber, Y. Liu, and D. Wang (2001), The advanced regional prediction system (arps) — a multi-scale nonhydrostatic atmospheric simulation and prediction model. part ii: Model physics and applications, *Meteorol. Atmos. Phys.*, *76*, 143–165.